

We are IntechOpen, the world's leading publisher of Open Access books Built by scientists, for scientists

6,900

Open access books available

185,000

International authors and editors

200M

Downloads

Our authors are among the

154

Countries delivered to

TOP 1%

most cited scientists

12.2%

Contributors from top 500 universities



WEB OF SCIENCE™

Selection of our books indexed in the Book Citation Index
in Web of Science™ Core Collection (BKCI)

Interested in publishing with us?
Contact book.department@intechopen.com

Numbers displayed above are based on latest data collected.
For more information visit www.intechopen.com



Nanoscale Methods to Enhance the Detection of Ionizing Radiation

Mark D. Hammig
University of Michigan,
USA

1. Introduction

The dominant modern methods by which ionizing radiation is sensed are largely based on materials that were developed decades ago, in the form of single crystal scintillators (such as sodium iodide (NaI(Tl))) or semiconductors (silicon (Si) or high purity germanium (HPGe) principally), and gas-filled counters (e.g. ^3He for neutron detection). These legacy materials have survived and flourished because they have delivered adequate performance for many medical imaging, military, and plant-monitoring applications, and there was no low-cost replacement materials that delivered equivalent or superior performance. Thus, most of the research effort throughout the latter half of the 20th century was focused on the implementation of single-crystal solid and gas-filled detectors into various radiation-detection niches.

The elevation of the concern over the threat presented by secreted radiological and nuclear-weapons has, however, driven a need for superior detection media. If one wishes to have the ubiquitous deployment of radiation sensors, then existing materials are unsuitable because they have either poor efficiency (Si), demanding logistical burdens (liquid nitrogen associated with HPGe), or unduly high cost (cadmium zinc telluride (CZT)). For simple *counting* applications, emerging solutions exist in the form of boron-coated straw based neutron detectors (Lacy, et al., 2010) and liquid scintillators; however, if high resolution imaging of the radiation field is to be accomplished, then one prefers a material that makes a highly accurate conversion of the particle's energy into the information carriers in the detection media.

The dominant sensing technologies of *ionizing* radiation depend on its namesake; that is, they sense the non-equilibrium charge states induced in the interaction media. Thus, either charges, in the form of electron-ion or electron-hole pairs, can be sensed by their effects on the electric field created by the surrounding device architecture, or the light that accompanies the radiative-recombination of that charge is monitored using scintillation photon detectors. Unfortunately, in the process of creating that charge, information is lost to phonon-creation which doesn't participate in signal formation.

One of the main motivations that drives the development of nanostructured materials, whether nanoscintillators or nanosemiconductors, is that the phonon-assisted loss-processes can be suppressed to a larger degree than is possible in single-crystal materials, such that more of the incident information is converted into the information carriers (charge, light) that participate in signal formation.

As we will discuss, realizing those properties requires careful control over: (1) the structure, size, and uniformity of the nanoparticles themselves, (2) effective coupling of the nanoparticles into a colloidal solid through which the information can flow unimpeded, and (3) suitable device design such that the information can be coupled into a readout circuit. Given the challenging tasks associated with deploying nanostructured media, one might ask whether one can eschew the charge-conversion modality altogether.

If the loss of information to heat is a challenge that requires careful control over the energy-band structure of the solid, why doesn't one just measure the heat directly with a sensitive thermometer? This, in-fact, is the approach that delivers the best energy-resolution currently achievable, in the form of microcalorimeters. In fact, the resolution is several orders-of-magnitude better than that produced by HPGe or the best nanocrystalline detectors. However, the temperature variations that accompany radiation impact are sufficiently slight that small detection-volumes bounded to superconducting readout circuits are required, whether one uses transition edge sensors (Ullom et al., 2007) or magnetic microcalorimetry (Boyd et al., 2009). Useful interaction rates can be achieved by multiplexed arrays of the underlying sensor, but the microcalorimetry technologies magnify the cost and logistical concerns associated with using HPGe detectors.

The second motivation for employing nanoparticle approaches is thus that high energy-resolution performance can be achieved with a lower-cost, larger-area alternative to detectors based on single-crystal materials. Although one can deploy high-vacuum, precisely controlled chamber-based equipment (e.g. molecular beam epitaxy) to create and grow nanoparticles, the most common approach is one of wet-chemistry, in which atmospheric pressure or low-vac processes are used to create the colloidal dispersions. Furthermore, the resulting solutions can then be deposited into solids of various form by the utilization of self-assembly during the solvent drying phase. Thus, the initial capital cost is far less than that required in a fabrication methodology based on microelectronic processing equipment, such as single-crystal growth furnaces. For instance, the current cost of deploying a cubic centimeter of the leading room-temperature single crystal semiconductor, CZT, is roughly \$1,000, while we estimate that an equivalent volume of a nanostructured lead-selenide detector can be deployed for less than \$10, based on labor and materials costs. In Section 2, we discuss some of those processing steps required to make the nanocrystalline detectors, and we show that they can produce excellent energy response utilizing large detection volumes.

As will be shown, experimental results reveal that structuring *semiconductors* in a solid nanocrystalline composite can suppress the heat-loss mechanism relative to charge-creation processes, resulting in better estimates of the initial energy of the radiation than those produced by single-crystalline materials. In principle, the uncertainty in the energy-measurement process can be reduced the size of the band-gap, which serves as the fixed increment that governs the number of charge-carriers created. However, we currently measure ~1 keV energy uncertainty rather than typical band-gap values of 1 eV, and substantial improvement must therefore be achieved to turn the principle into practice. In fact, the precision of the nanosemiconductor is such that much of the uncertainty is governed by the electronic noise of the readout circuit, but if that is quenched, then one expects the measurement uncertainty to be governed by the non-uniformities in the underlying material.

One might ask: can one do better even than the uncertainty produced by the *electronic* band-gap? Microcalorimetry provides one pathway because information-carrier creation is

governed by the phonon energy structure. One can also utilize sensors which gauge the momentum of the incident particle, and therefore avoid the energy-loss pathways inherent to energy-conversion devices, as summarized in (Hammig et al., 2005). In fact, *mechanical* radiation detectors are close cousins to microcalorimeters because small detection volumes must be cooled to quench competing thermal noise sources, and arrays of sensors must be deployed to realize large detection efficiencies. However, holographic methods can be brought to bear to read-out an array of vibrating elements in parallel.

When capturing the incident radiation and transforming its physical parameters into a measurable quantity, modern sensing technologies of *neutral* particles depend on an abrupt modality, in which the impinging photon or neutron is converted into a secondary charge-carrier in a point interaction, which subsequently generates heat, charge, or momentum during its slowing in the detection medium. One might prefer to avoid the point conversion altogether and take advantage of the wave-mechanics of the incident particle. In Section 3, we will discuss some of the proposed methods by which radiation can be guided and bent such that its inherent information is not processed through inefficient information-carrier creation processes.

2. Nanosemiconductors

2.1 Why not nanoscintillators?

For nanostructured media, the dominant modality currently being investigated by the radiation-detection community consists of composite arrays of nanoparticles that scintillate upon their excitation. The physics motivation is that in comparison to single crystalline materials, nanostructured scintillators exhibit: (1) enhanced light emission due to the suppression of non-radiative loss processes, and (2) more rapid emission kinematics due to a higher degree of intradot charge coupling, both of which yield higher imaging performance. Nanoscintillators consisting of lead-iodide (Withers et al., 2009), rare-earth-doped fluorides, such as $\text{CaF}_2(\text{Eu})$ and $\text{LaF}_2(\text{Eu})$ (Jacobsohn et al., 2011), and rare-earth oxides, such as LuBO_3 (Klassen et al., 2008) among many other materials are currently being studied, many exhibiting accelerated decay responses and high light conversion efficiency on a nanoparticle basis.

The main challenge presented by the composite media is the optical self-absorption in the nanoparticles, the matrix, and the innumerable interfaces as the photons meander their way to the readout surface. To date, no nanocrystalline scintillator detector has exhibited comparable characteristics to the best single-crystal media, whether composed of $\text{NaI}(\text{Tl})$ or brighter scintillators such as $\text{LaBr}_3(\text{Ce})$. More to the point, one doesn't anticipate that an optimized light-emission media will ever produce a greater number of information carriers than a semiconductor equivalent because of the losses associated with converting the charge into scintillation light- and back again, at the photocathode or photodiode readout.

Thus, our initial investigations have been into nanosemiconductor composites, in which we have determined if one can overcome their expected limitations; namely, (1) charge loss during the slowing-down of the charged-particle in the matrix, (2) charge trapping during subsequent electron and hole transport, and (3) small detector volumes.

Regarding the latter point, small thin detectors typically accompany nanosemiconducting devices because of the inevitable colloidal defects that accumulate as a greater number of layers are cast onto the sample. Furthermore, biasing the device such that a high electric field is realized throughout the volume can, *a priori*, be challenging because of either poor

Schottky junctions or low-resistivity substrates. One might reasonably anticipate that depleting several centimetres of charge might be impossible without high bias voltages. Fortunately, these reasonable expectations are not met and sizable detector volumes can be realized over which rapid, clean charge transport can be achieved, as we will discuss next.

2.2 Cadmium telluride NC detector responses

Lead chalcogenide (PbS, PbSe, and PbTe) quantum dots have favorable properties for their use in NC applications. In contrast to a colloidal cadmium salt, such as CdTe, the large bulk Bohr radii of its excitons (e.g. 46 nm for PbSe) enables strong quantum confinement in relatively large NC structures. Since the conductivity improves sharply as the degree to which the particles are both mono-disperse and close-packed (*cf.* Remacle et al., 2002), larger particles result in better charge transport because the growth techniques are approaching the precision corresponding to the addition of an atomic layer. Another relative advantage of lead chalcogenides compared to CdTe is the nearly identical and small effective masses of the electrons and holes that can be attributed to the symmetric structure of the conduction and valence bands, which gives rise to relatively simple and broadly separated electronic energy levels that in turn, leads to much slower intraband relaxation (Schaller et al., 2005). Moreover, previous studies on lead chalcogenide NCs have shown that these materials have unique vibration states, weak electron-phonon coupling, and negligible exchange and Coulomb energies; thus, they have temperature-independent energy band-gap (e.g. Du et al., 2002; Olkhovets et al., 1998).

Our main focus therefore lies with the lead salts. However, the cadmium chalcogenides have, at present, more mature fabrication recipes and more importantly, their bulk band-gap is higher- 1.44 eV for CdTe compared to 0.26 eV for PbSe. This latter point is important because for low ($< \sim 1$ eV) band-gap semiconductors the fluctuations in the thermal noise compete vigorously with the small energy depositions that accompany radiation interaction, and they can swamp the measurement so that x-rays and low-energy particles are unresolvable.

2.2.1 Detector fabrication

CdTe is a II-VI semiconductor material that has been extensively investigated as a single-crystal semiconductor radiation detector. NCs of cadmium chalcogenides are also widely studied for the detection of optical photons. In fact, the fabrication methods are geared toward thin films consistent with the stopping of non-ionizing poorly-penetrating radiation. Although less favorable than the lead chalcogenides for the intended application, the synthesis processes are more fully characterized, and we have therefore investigated both systems.

One method to produce monodisperse NCs involves the mixing of all the reaction precursors in a vessel at a low temperature and then moderately heating the solution to grow the particles. An accelerated chemical reaction induced by increasing the temperature of the solution gives rise to supersaturation, which is relieved by the nucleation burst. The subsequent control of the solution temperature will induce further growing of NCs (Kim et al., 2009).

For instance, NCs in the ~ 3 nm range can be grown in 20 minutes, whereas larger particles can take 24 hours or more, the size judged during growth via the UV-photoluminescence.

For instance, a synthesized NC dispersion may exhibit green-colored photoluminescence of 540 nm average wavelength, which corresponds with a NC particle size of 3 - 5 nm. According to the chemistry of the synthetic process, the resulting dispersion contains NCs with a CdTe crystalline core surrounded by deprotonated -OH and -COOH groups of the thioglycolic acid; thus, the NCs have negative charge (Rogach, 2002).

For electronic testing, assemblies composed of ~4 nm NCs were prepared by two methods: the layer-by-layer (LBL) method and via drop-casting the NC dispersion on aluminum and gold-metalized glass substrates. The LBL method is a well-known method for efficiently depositing NC colloidal dispersions into high quality and stable thin-film layers on the substrate, while preserving the distinctive optoelectrical and magnetic properties of the size-quantized states of the NCs. For the LBL deposition, poly(diallyl dimethyl ammonium chloride) (PDDA), was induced as a polycation used for adsorbing nanoparticles. Thioglycolic-acid (TGA)-stabilized CdTe nanocrystal solution was spread on the PDDA layer and adsorbed. By an alternatively adsorbing procedure, a bilayer consisting of a polymer/nanocrystal composite was developed and the cycle was repeated from 1 to 30 times, to obtain a multilayer film of the desired thickness.

Unfortunately, in order to stop the high-energy charged particles associated with ionizing radiation one desires a thickness of at least 10's of micrometers if not several centimeters, which requires repetitive and lengthy casting procedures; for instance, roughly 80 hours of aqueous layer-by-layer deposition is required to achieve 10's of micrometers thickness. This can be enabled by robotic dipping tools, but for characterization studies, one can utilize sub-micrometer layers to evaluate the material.

The result of spin-casting the NC assembly onto a glass 4" diameter wafer is shown in Fig. 1A. The varying color reflects the non-uniform thickness deposited towards the outside of the wafer. If the uniform, inner-section of the assembly is diced and bounded by metallic electrodes, then 1 x 1 cm² detectors can be realized, as shown in Fig. 1B. In order to determine the thickness of the resulting NC assembly, we examine the cross-section of the layer and utilize energy dispersive x-ray spectroscopy to identify the constituent layers, as shown in Fig. 2. Note that the gold, indium, and cadmium signals overlap but a careful examination of the various structures reveals that the layer is only 130 nm thick, achieved after 48 drops of the LBL process was repeated (cf. Fig. 2C).

2.2.2 Spectroscopic ion measurements

A priori, one expects only slight energy depositions within a 130 nm layer, particularly for weakly ionizing electrons. Even if one exposes the assembly to 5.485 MeV alpha particles (from ²⁴¹Am), the energy deposited from the transmission of the ion through the layer is less than 30 keV. This is enough energy to produce a measurable signal, as shown in Fig. 3, which is very promising because gamma-rays, for instance, can produce energy depositions that are 10 times as big if there is enough volume to fully stop the products of the interaction.

Thus, even though the cadmium salts may not be as favorable as their lead equivalents- at least in their physics properties- they represent a promising material upon which nanostructured ionizing radiation detectors can be developed. Furthermore, detectors fabricated using the LBL method are more reproducible in their behavior than those that are solidified using gross drop- or spin-casting methods.

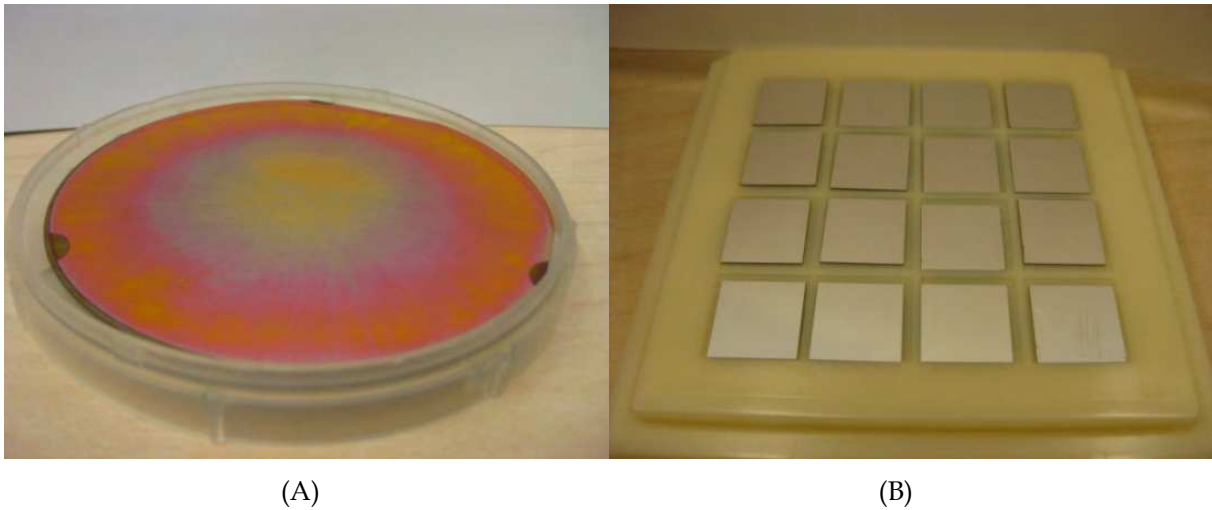


Fig. 1. (A) Gold-metalized glass wafer upon which a colloidal dispersion of CdTe NCs is deposited via the LBL method utilizing spin-casting. (B) The 1 x 1 cm² detectors after indium evaporation and dicing.

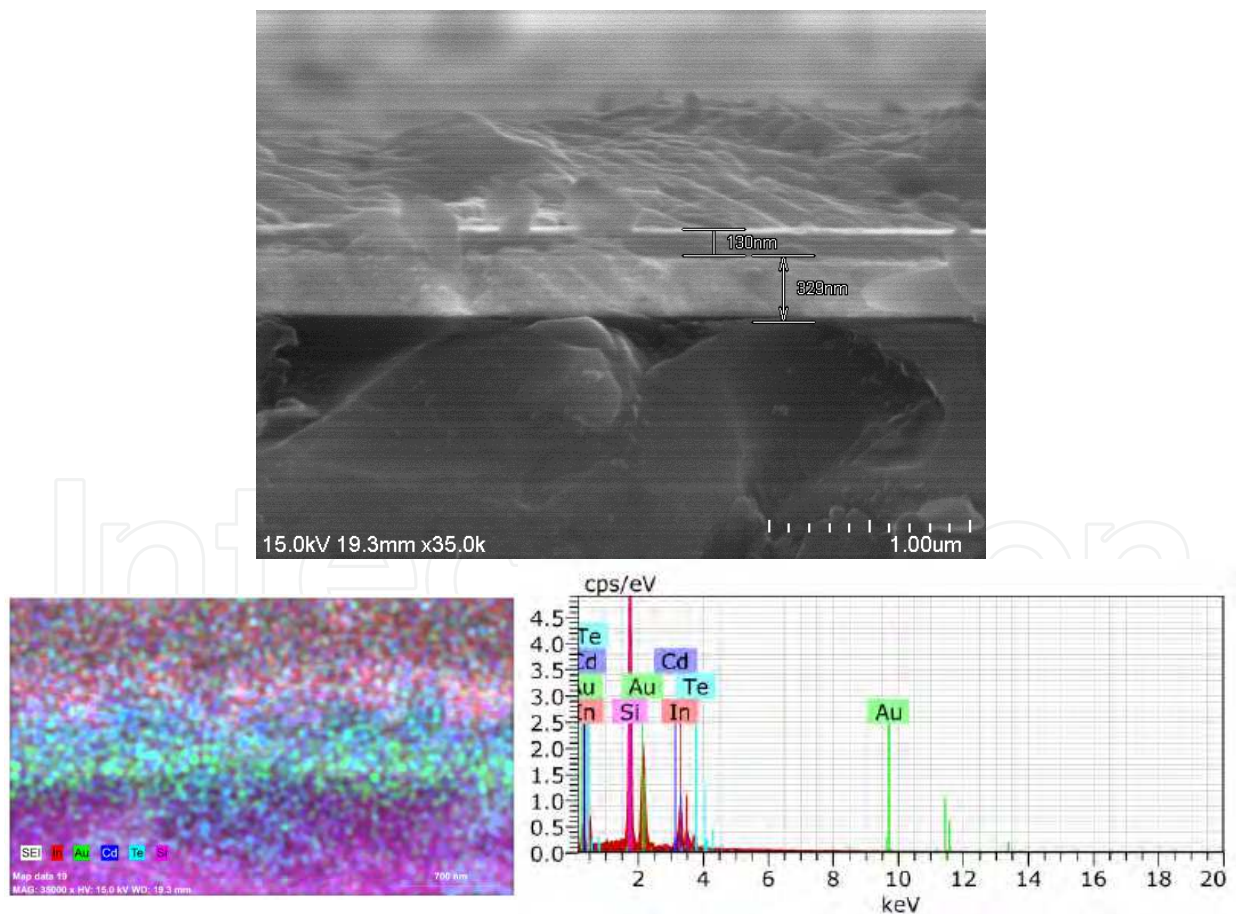


Fig. 2. (A) SEM micrograph of a cross-section of the NC CdTe detectors, showing the 329 nm gold layer and 130 nm CdTe assembly, assignments verified using energy dispersive x-ray spectroscopic mappings of (B) and (C).

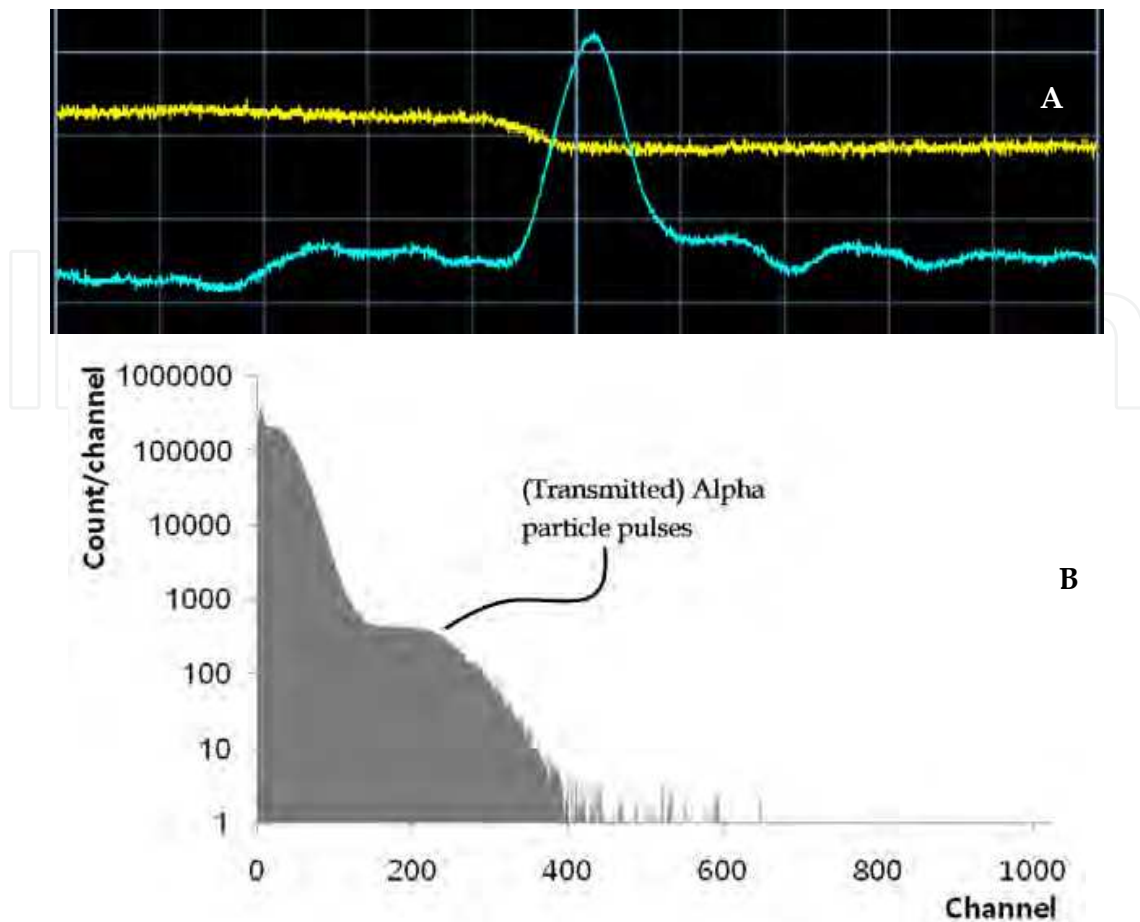


Fig. 3. (A) Preamp (yellow) and shaped (blue) signals derived from the passage of a 5.485 MeV alpha particle through a 130 nm CdTe nanocomposite detector, in which the induced charge signal is measured with a Ortec 142A preamp. The time per division is 10 μ s and the volts per division are 200 mV for the preamp and 5 V for the shaped pulse. (B) An example alpha particle spectrum in which the alpha pulses are shown as a hump above the noise.

Nevertheless, instead of using the dozens of hours required to grow detectors with good intrinsic detection efficiency, one can produce exceptional detector behavior using chemistry based on fast-drying organic solvents and through deposition procedures that result in detectors that can be realized in minutes instead of hours. Furthermore, the lead salts, with their higher atomic numbers and densities, have inherently higher stopping power to either charged or neutral ionizing radiation, as shown next.

2.3 Evaluation of the relative efficiencies of competing materials

Fig. 4A shows that when one compares various common single-crystal detection media and the lead chalcogenides under study, PbSe and PbTe in both single-crystal and nanocrystalline form are superior in terms of their combined mass densities and atomic numbers, Z , both of which combine to yield a higher specific detection efficiency.

The nanocrystalline forms of PbSe and PbTe are consistent with some of our current colloidal solids, in which spherical 10 nm PbSe nanoparticles or spherical 5 nm PbTe dots are spun cast into a face-centered-cubic (FCC) nanocrystalline solid with an interstitial para-MEH-PPV polymer of order 1. In realized detectors, we vary the relative blending of the

polymer and NCs such that higher polymer orders are typically employed, and we grow rods and cubes, as well as spheres. Furthermore, the geometry of the solid deviates from a perfect FCC structure to a degree depending on the size dispersion of the colloidal solution; nevertheless, the reduction in densities between the single-crystal lead chalcogenides and the nanocrystalline forms reflects the values that are achieved when the ordering and spacing are optimized for spherical NCs. As shown in the figure, even in nanocrystalline form, the lead chalcogenides maximize the probability of interacting with impinging high-energy photons, and more generally, they exhibit superior characteristics for the efficient stopping of primary or secondary charged particles.

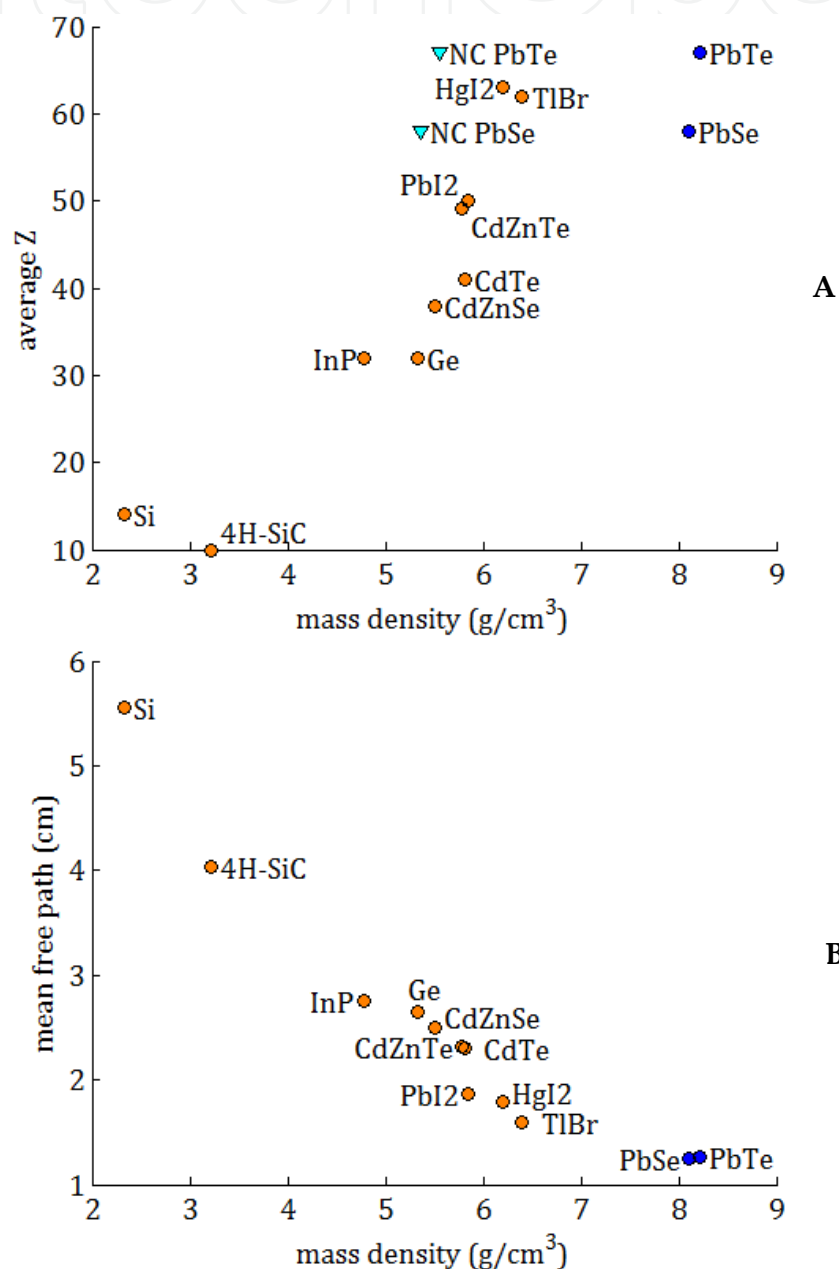


Fig. 4. (A) Relationship between the average atomic number Z and the mass density for various semiconducting materials. (B) The mean free path for a 662 keV photon interacting with single-crystal forms of the semiconducting media (Hammig & Kim, 2011).

As an example, Fig. 4B shows the photonic mean free path, as derived from the density and the macroscopic *photoelectric-absorption* linear attenuation coefficient at a photon energy of 662 keV, which is consistent with the gamma-ray emission from ^{137}Cs . A comparison of PbSe or PbTe with CZT- the most common room-temperature gamma-ray detection medium- shows that the mean free path in CZT is 1.85 times longer than that of either lead salt. On a path-length normalized basis therefore, the lead chalcogenides can form a highly efficient gamma-ray detection medium. Nevertheless, the question is: in a field in which device thicknesses are measured in nanometers to hundreds of nanometers, can the solid be formed into electronic structures with enough active thickness and lateral extent to take advantage of the inherently high interaction probabilities and stop charged particles that may range over hundred of micrometers? As described in Section 2.41, the drop-, dip- and spun-cast solids can be formed into thicknesses which yield highly efficient detector configurations.

One not only desires high probabilities of interaction with the incident quanta, but the multiplicity of the subsequent charge-creation should be maximized and the trapping of the charge-ensemble should be minimized so that the information conversion is optimized. As summarized in Section 2.42, the charge transport can vary across the lateral area as well as in depth because of the varying field or mobilities that accompany different packing regions. Nevertheless, one can bias the detector such that the charge velocities are saturated, resulting in uniform collection across the ensemble.

As shown in Section 2.43, even with a colloidal solid that is not optimized from a charge-separation and transport perspective, the resulting energy-resolving behavior is comparable to or better than state-of-the-art single-crystal semiconductors- Si, CZT, and high-purity germanium operated at liquid nitrogen temperatures- which reflects the promise of the nanostructured approach to semiconductor device design, extending beyond the sensing application reported.

2.4 Lead selenide NC detector responses

2.4.1 Detector fabrication

The chemical recipe used to form the colloidal dispersion, the subsequent characterization of the nanoparticles, and their formation into solid assemblies is described in (Kim & Hammig, 2009). Colloidal PbSe NCs were synthesized through the high-temperature solution-phase routes (Murray et al., 2001), as illustrated in the Fig. 5. Lead oleate and selenide-dissolved trioctylphosphine (TOP-Se) were used as the organo-metallic precursor and diphenyl ether (DPE) as the high-temperature organic solvent. The lead oleate precursor was prepared by dissolving lead acetate, $\text{Pb}(\text{CH}_3\text{COO})_2$, into a mixture of DPE, TOP and oleic acid, heated up to 85 °C for 1 hour and cooled down. Mixed with 1 M TOP-Se solution, precursors were rapidly injected into rigorously stirred DPE at various reaction conditions (T_{inj}) in an inert environment. PbSe NCs were grown in T_{gr} for 3 - 6 minutes and cooled.

In the fabrication of the NC assembly detector, one forms a mold in an inert substrate which acts as a basin into which the colloidal dispersion is dripped. Furthermore, both the top and bottom metal contacts must be accessible in order to connect each face of the detector to the readout electronics. Although we have used silicon, printed circuit board, glass, and plastic substrates, we typically use glass substrates for thin detectors (10's of micrometers to 100's of micrometers) and employ plastic substrates for millimeter or centimeter thick devices. Fig. 6 shows the typical process if a glass substrate is used, which makes use of standard photolithography processes.

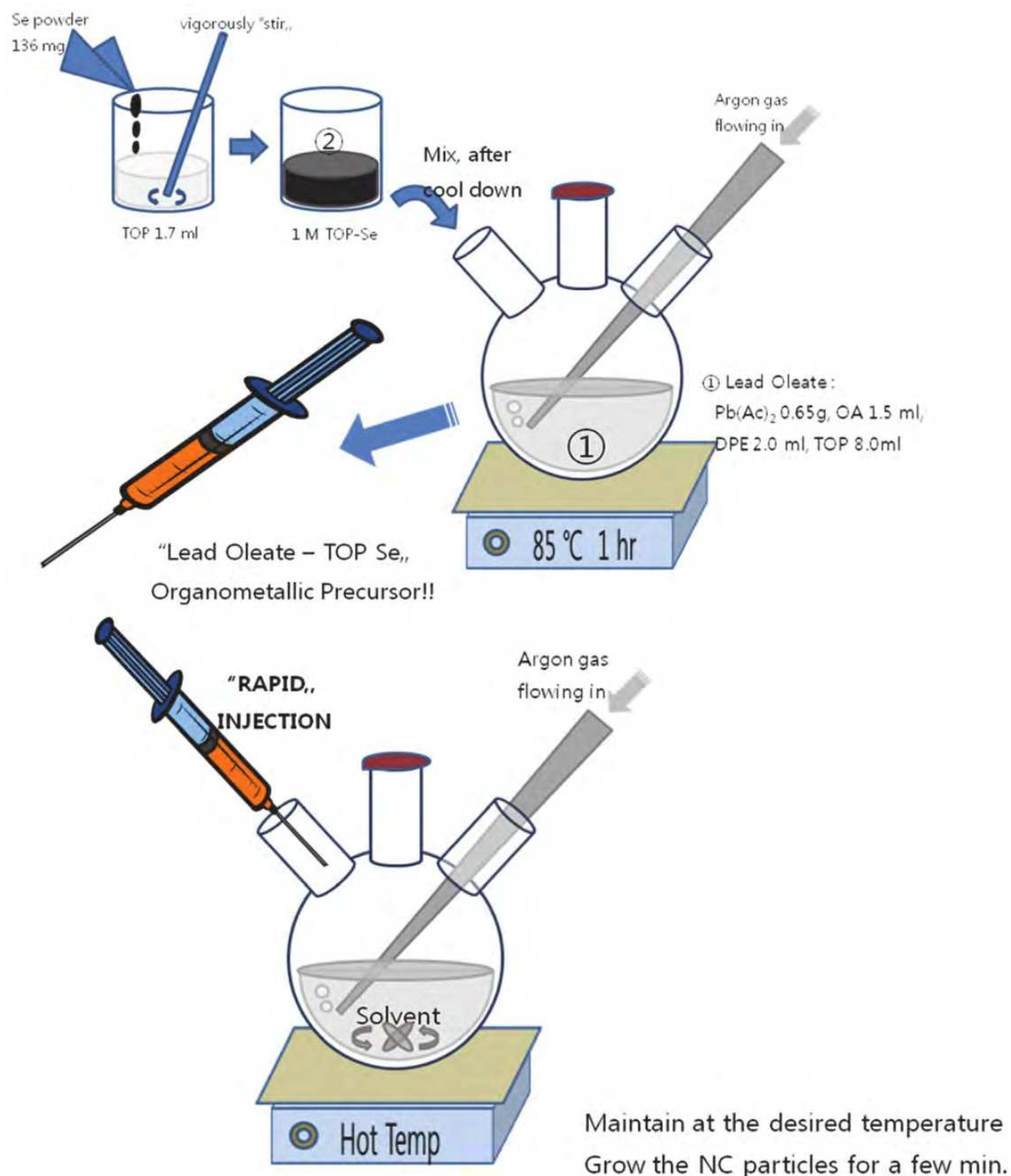


Fig. 5. Schematic of the PbSe NC dispersion synthesis.

Several fabricated substrates are shown in the Fig. 7. The lines stretching horizontally and vertically are due to the dicing of the substrate. Blue colored tape is attached to the backside, before the substrate is diced. The glass wafer-based substrates were designed in a circular shape to make the spin-casting procedure more efficient. Once the metalized molds are realized, the NC assembly can be deposited to form the active region of the sensor.

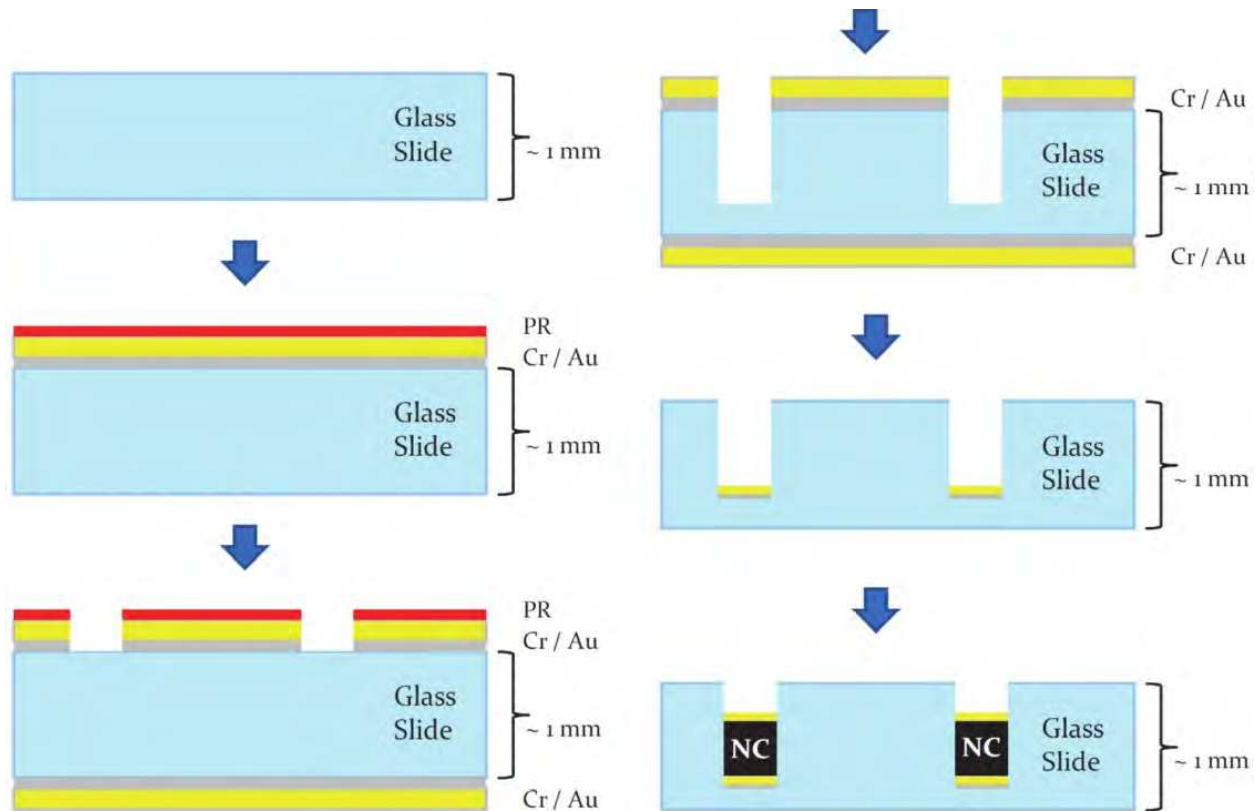


Fig. 6. Schematic of glass wafer-based NC assembly substrate fabrication procedure.



Fig. 7. Glass wafer-based NC assembly substrate with Al and Au bottom contacts.

Synthesized NC particles inherently self-assemble, if coordinated with organic ligands properly. NC particles dispersed in the chloroform solvent can be deposited on the substrate using many methods, but we have focused on drop- and spin-casting. Drop-casting is the process of depositing a droplet of the NC solution on the substrate and repeating the procedure, while allowing time for the solvent to evaporate between applications. Spin-casting is the process of dripping a droplet of the solution on a spinning substrate, which allows more uniform spreading of the NC solution as well as more rapid drying.

In order to realize suitable charge transport, the PbSe NC solution is mixed with a conductive polymer, for instance, para-MEH-PPV, which is used as a hole transporting agent. Greater polymer concentrations formed a brighter, more yellow assembly, whereas the pure PbSe NC assembly exhibits a dark assembly, as shown in Fig. 8 and Fig. 9. Note that Fig. 9 shows the assemblies deposited into ~5 mm deep holes with 7 mm diameters milled into plastic substrates, and the detectors therefore form active depths that are several millimeters thick.

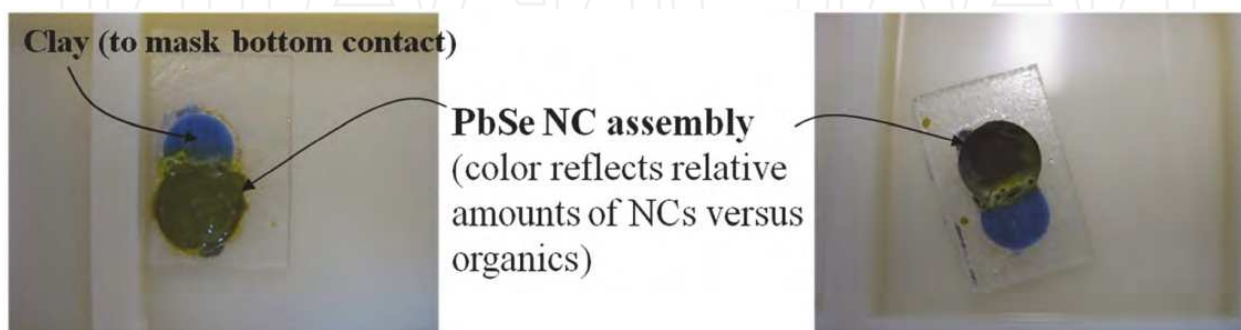


Fig. 8. PbSe NC/MEH-PPH composite assembly deposited on the glass substrate.



Fig. 9. PbSe NC/MEH-PPH composite assembly deposited on plastic substrates, before the top metal contact is formed (left) and after gold evaporation (right).

Various metal contacts can be used to abut the NC assembly, in which the band-structure can vary significantly with the particle size. In general, the MEH-PPV is p-type and we therefore use metal contacts with higher work functions, such as Pt (5.6 eV) and Au (5.2 eV), for the ohmic contact, and we form the rectifying contact with lower work function metals, such as In (3.8 eV) and Al (4.2 eV). Various combinations of samples were made in order to study the effects of the metal contacts, including Pt/NC/Pt, Pt/NC/In, Au/NC/Au, Au/NC/In, etc.. Nevertheless, the behavior of the resulting detector does not depend strongly on the bounding Schottky barrier; rather, the charge creation and transport is more dependent on the uniformity of the colloidal solid underlying the electrodes, some features of which will be described next.

2.4.2 Charge transport characteristics

As mentioned in Section 2.2, a close-packed solid with a high degree of size uniformity results in high conductivity. The size-dispersion in the NC solution depends on procedures used to prepare the liquid dispersion of coordinated-NCs. One can achieve monodisperse (particle size with less than 5 % uncertainty) solutions either directly from the nucleation and growth procedure- with finely controlled reaction conditions- or by employing size-selective precipitation procedures. For instance, Fig. 10 shows the size separation for CdTe NCs that can be elicited using incompatible and compatible solvents along with centrifugation, into a size-stratified solution (Fig. 10A). The separated layers (Fig. 10B) then exhibit different particle size via their size-dependent band-gap in their color or in their excitation spectra. The size can be further refined by repeated application of the procedures if needed.

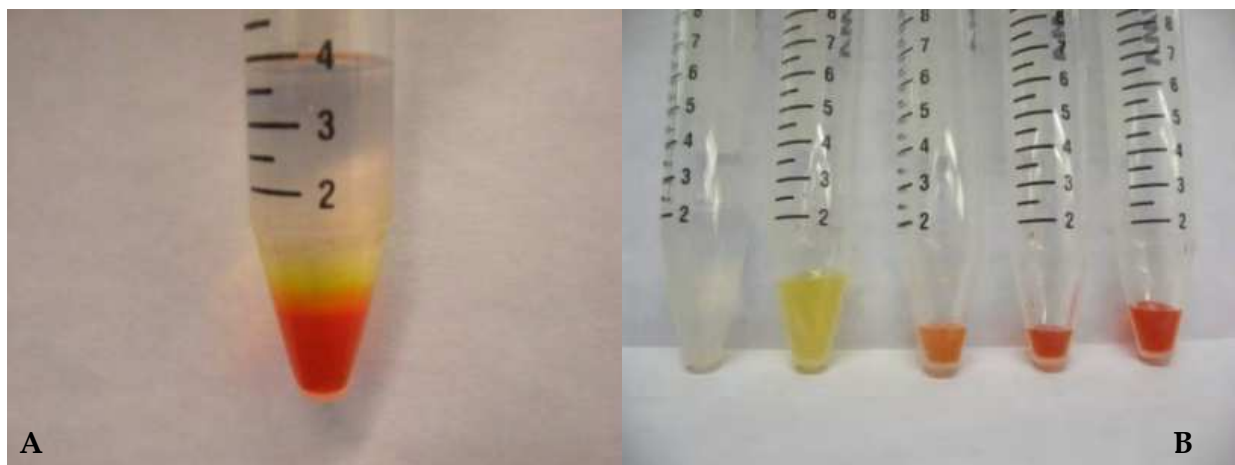


Fig. 10. (A) The separation of a CdTe NC dispersion (with size range in the 3-5 nm range) into different precipitation bands following centrifugation. (B) The separation of the bands into different vials through pipetting.

The importance of monodispersity is not only in the electrical characteristics but in the mechanical ordering properties (Coe-Sullivan et al., 2005). A large ($> 10\%$) distribution in size results in random packing, but narrow distributions that approach the uncertainty due to the addition of an atomic layer ($< 5\%$) result in high degrees of order.

Over microscopic areas therefore, monodispersity and the coordination chemistry can be employed to realize close-packed assemblies. However, when one examines the solid over larger volumes, then defects are apparent, ranging from quantum dot (QD) crystal defects, such as vacancies and dislocations, to large-scale cracks, such as those shown in Fig. 11. The large-scale cracking, which we see in all of our samples is a natural consequence of stress-relief during drying of the solvent. The formation of domains of differing degrees of NC order can be reflected in the charge transport characteristics.

For instance, if the bias is held low enough (a value depending on the diode design), then Fig. 12 shows that following the interaction of a single quanta, the holes move in fits and starts, as reflected in the induced charge pulses (in yellow) along with their amplified and shaped counterparts (in blue). This reflects an underlying variation in the drift velocity as the charge cloud traverses different depths of the active volume, with can be caused by either variations in the electric field or the mobility. Although these variations could

potentially be problematic if one were to use pulses such as those shown in Fig. 12 to extract the energy deposited by the radiation, one can increase the voltage such that all of the slow-drift regions are eliminated, and the pulse rises sharply and cleanly, such as that shown in Fig. 13. One explanation for this behavior is that the charge-velocities saturate across the various domains in the NC detector and the transport variations are therefore of no consequence.

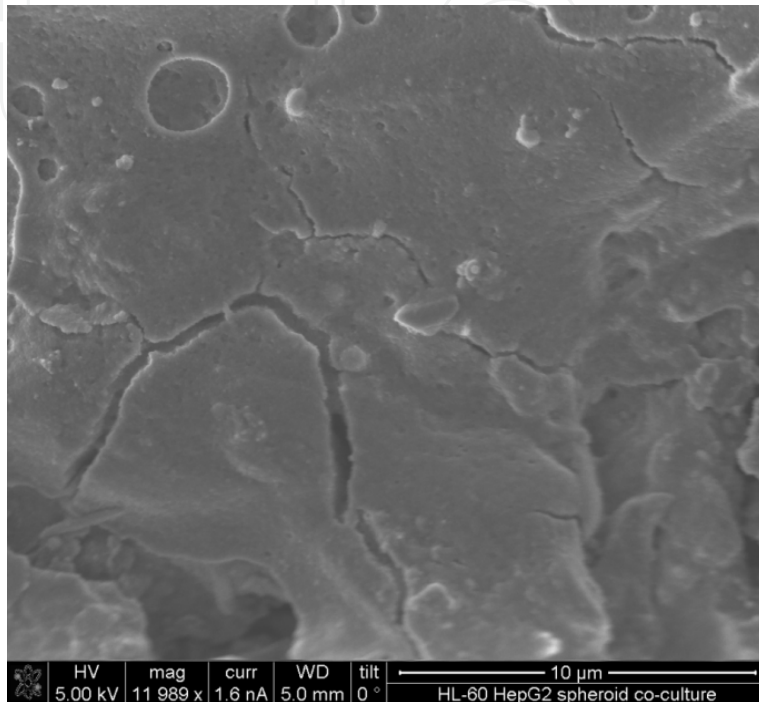


Fig. 11. The cracked and stacked dried mud-puddle look of the NC assembly at a scale of 10's of micrometers.

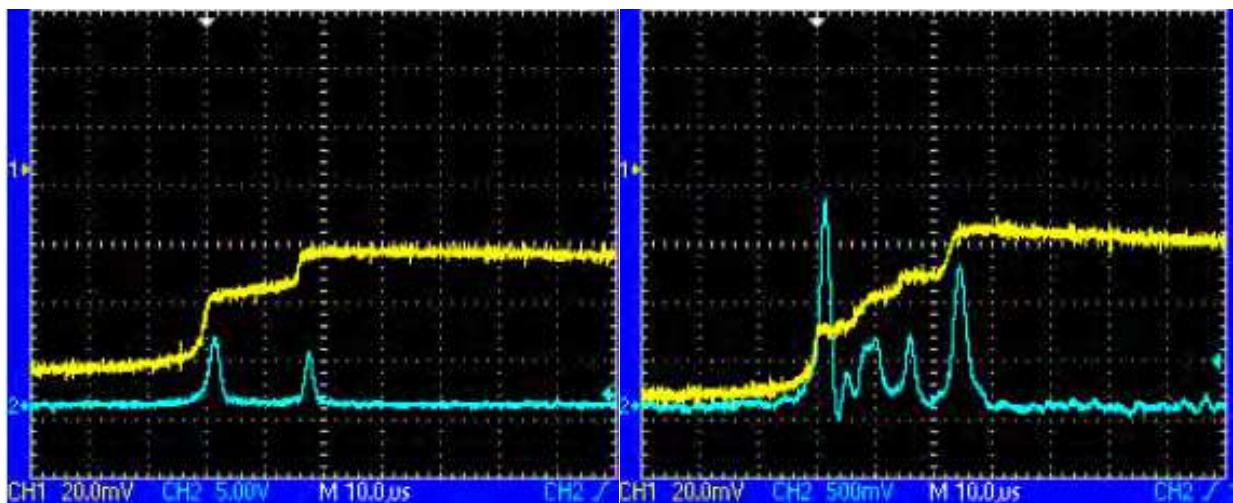


Fig. 12. Two examples of preamp (yellow) and shaped (blue) signals derived following the stopping of an ^{241}Am alpha particle within an under-based colloidal PbSe detector.

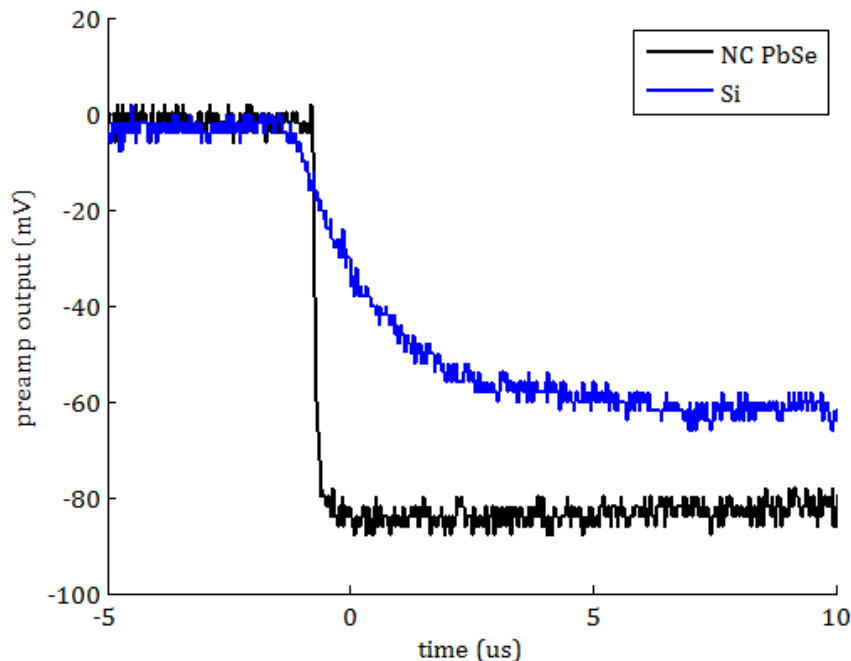


Fig. 13. The pulse shape derived from the charge-sensitive preamplifier (Ortec 142a) when an alpha particle from ^{241}Am is impinged upon a silicon PIN or NC PbSe detector, both operated at 0 V applied bias. The PbSe nanoparticles are spherical with a mean diameter of 7.4 nm (± 0.5 nm).

Thus, although the dispersion is not monodisperse and the solid is not uniform, the promise of the nanocrystalline approach is revealed in the fact that the results are comparable to or better than state-of-the-art single crystal detectors, as will be shown next.

2.4.3 Spectroscopic measurements

Fig. 14A corresponds to a mixed spectrum derived from alpha particles- emerging from a *thin-film* ^{241}Am alpha particle source and ^{133}Ba gamma-rays impinging upon the 1 x 1 cm detector shown in Fig. 14A. The alpha source, placed 3.7 cm away from the detector surface, attenuates the 5.49 MeV particles to the energy range shown, and the ^{133}Ba source was placed external to the box housing the detector, 5 cm distant. If one focuses on those spectral features whose appearance correlates to the presence of the ^{133}Ba source, then we can identify the features using both the pulse amplitude and the frequency of occurrence as follows.

Although the material need not be linear, the pulse amplitudes of the full-energy gamma-ray peaks were linearly related to the energies identified in Fig. 14B. Second, the areas under the spectral features correspond to the expected values. For instance, if one takes the gamma-ray emission yield as well as the photoelectric absorption probabilities into account, the area of the 383.85 keV peak should be 12 % of that under the 356.02 keV peak, compared with a measured value of 11 %. The sizes of the x-ray escape features diminish for thicker detectors; however, the thin detector was utilized to characterize the charge-creation characteristics, minimally adulterated by charge-loss considerations, so that the inherent physical properties could be better estimated.

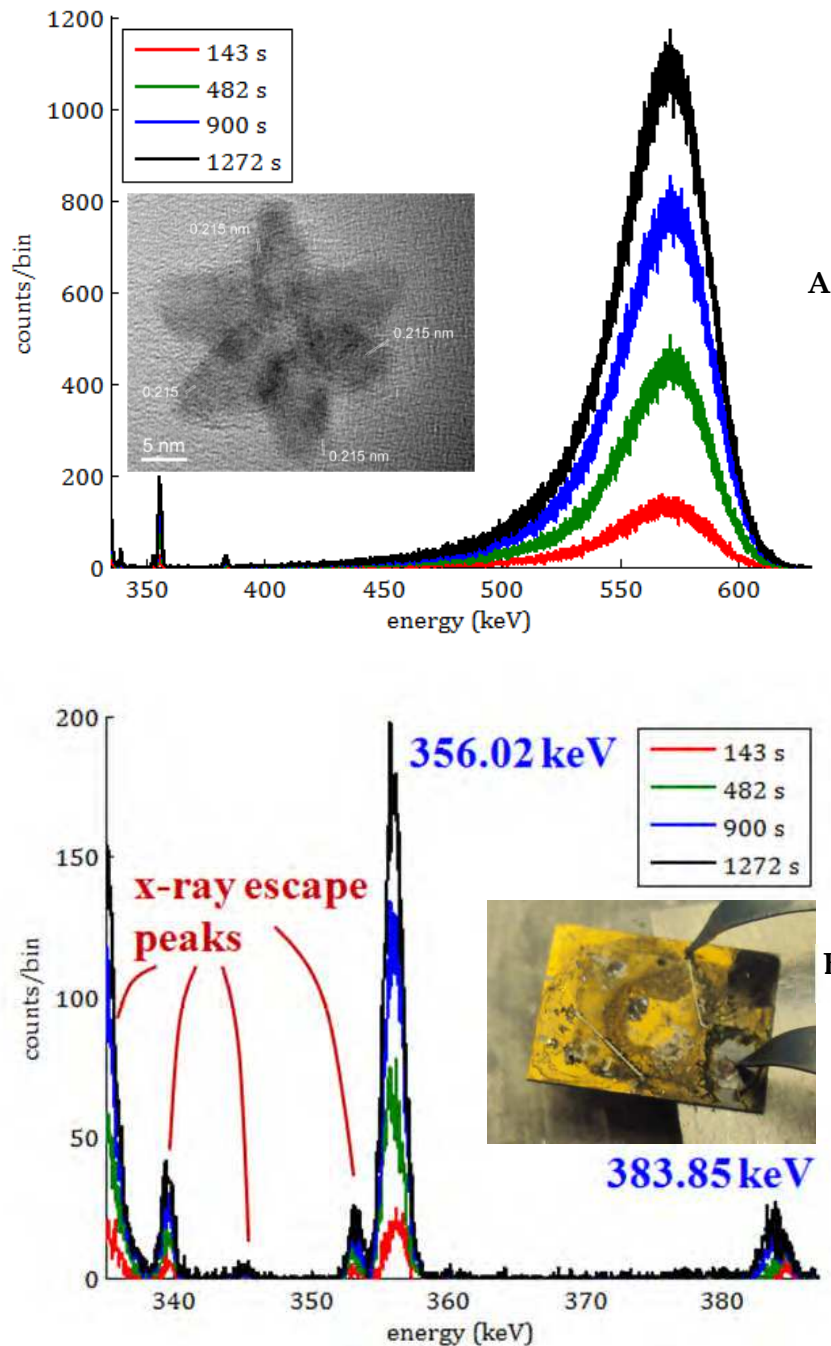


Fig. 14. (A) Energy spectrum derived from ^{133}Ba gamma-rays and ^{241}Am alpha particles, attenuated through 3.7 cm of air, impinging upon a 1 x 1 cm thin (10's of micrometers) composite assembly of para-MEH-PPV and star-shaped PbSe nanoparticles, accumulated for various durations shown in the legend. The inset shows a TEM micrograph of a typical PbSe NC in the assembly. (B) Typical ^{133}Ba spectrum derived from a thin detector, in which the Pb and Se x-ray escape peaks are prominent.

As reported in (Hammig & Kim, 2011), Fig. 15 shows the spectral widths compared with three state-of-art detectors, all operated at room temperature except for the high purity germanium (HPGe) detector, which was cooled with liquid nitrogen.

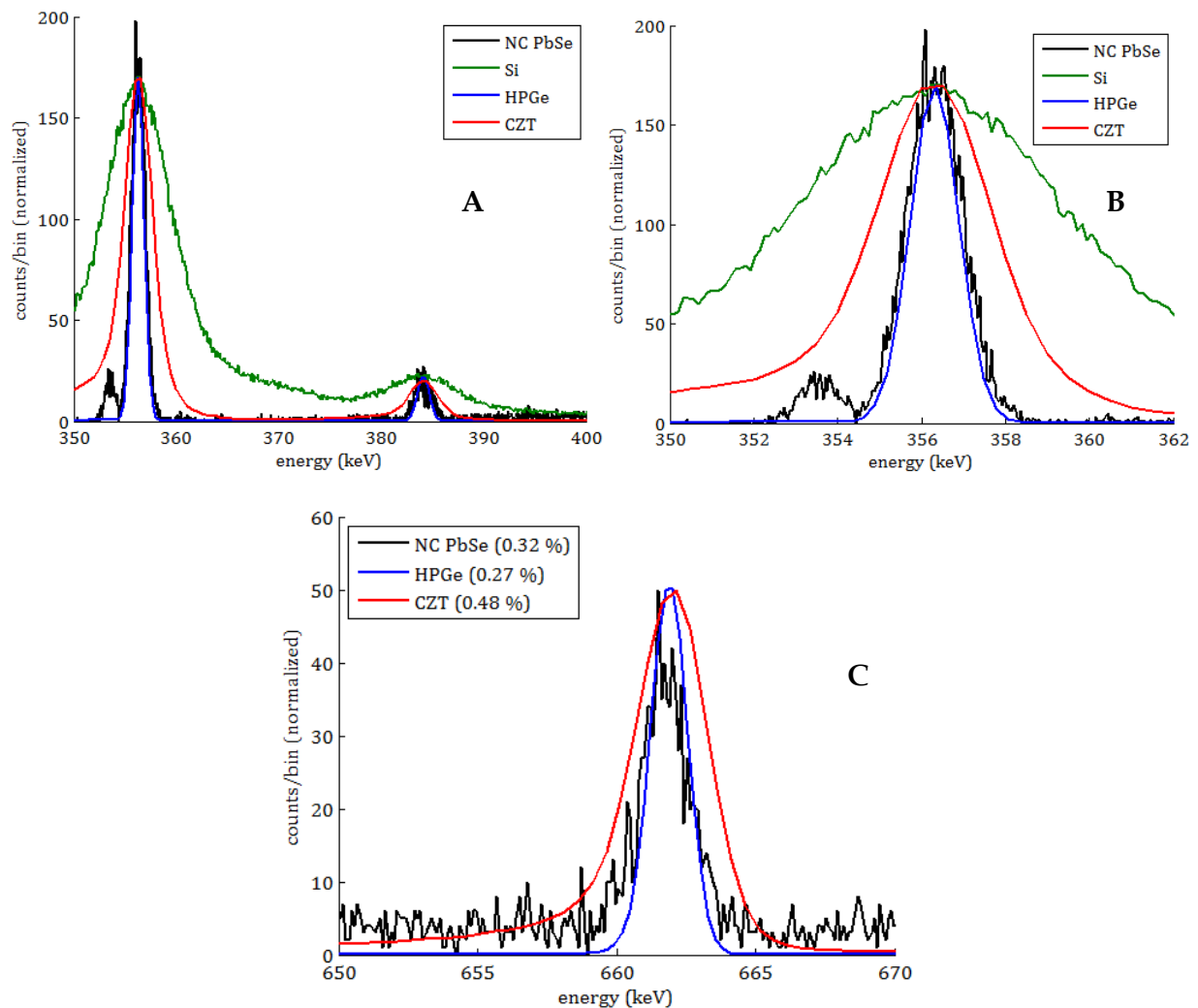


Fig. 15. (A) Spectral comparison between high-resistivity silicon (green), CZT (red), HPGe (blue), and the PbSe nanocomposite (black), when exposed to gamma-rays emitted from ^{133}Ba . The different measurement periods (e.g. 21.2 min for NC PbSe, 24 hr for HPGe) account for the differences in curve smoothness, and the curves were normalized to the number of counts in the PbSe peak. Note that the HPGe and NC PbSe traces largely overlap except for the x-ray escape peak from the NC PbSe detector. (B) Close-up of the 356.02 keV peak. (C) Spectral comparison between CZT (red), HPGe (blue), and the PbSe nanocomposite (black), when impinged upon by gamma-rays emitted from ^{137}Cs . The energy resolutions are shown in the legend. The measurement period for the NC PbSe spectrum was 46.4 min. (Hammig & Kim, 2011).

As shown in Figs. 15A and 15B, the energy resolution of the PbSe nanocomposite is superior to silicon and CZT and comparable to HPGe, yielding an energy resolution of 0.42 % (1.5 keV) at 356 keV, compared with a resolution of 0.96 % (3.4 keV) for CZT and 0.39 % (1.4 keV) for HPGe. Fig. 15C shows an equivalent comparison between the detectors when impinged upon by 661.7 keV gamma-rays from ^{137}Cs . The ^{137}Cs source was more than one hundred times less intense than the ^{133}Ba source and the peak was therefore less well sampled. More importantly, a slight gain drift in the detector dominated the peak width shown in the figure. Nevertheless, the ^{137}Cs results buttress those derived from ^{133}Ba

gamma-rays; namely, the nanocomposite detector provides an energy estimate with similar fidelity to that produced by HPGc. The results imply that the conductive polymers are not only accomplishing the goal of realizing good charge transport through the device, but they are not substantially participating in the charge loss of the recoil electrons.

2.5 Summary

Nanostructured cadmium and lead salts have been extensively studied as advanced media for optoelectronic devices. The sensitivity of their charge-transport properties to the surface conditioning of the nanoparticles and their degradation under ambient conditions has discouraged their use in a semiconductor configuration; rather, most of the efforts geared toward nuclear radiation detection have concentrated on nanostructured *scintillation* materials. Furthermore, the slight thicknesses that accompany the traditional spin-, dip-, and drop-casting methods have argued against their use as sensors of more highly-penetrating radiation.

However, we have shown that detectors with deep depletion regions can be constructed such that the deposited charge can be effectively drifted and the energy of the interacting quanta can therefore be measured. Furthermore, the accuracy of that measurement is comparable to those estimates provided by the best single-crystalline semiconducting materials, providing evidence for enhanced charge multiplication as the degree of strong confinement is increased.

Nevertheless, if one does employ thin detectors, then they are susceptible to the escape of the primary or secondary charged particles induced by the radiation's interaction, particularly for neutral particles that interact with roughly equal probability throughout the interaction depth of thin stopping media. The low energy tailing in the spectral features that are inherent to this energy loss can negatively impact the ability of the sensor to extract the physical characteristics of the impinging quantum, but more importantly, small volume detectors are inefficient for highly penetrating particles.

For neutral species, one might prefer to avoid the abrupt modality altogether, in which the particle is first converted into secondary charge particles which then confer the incident particle's information via electromagnetic interactions. If one can take advantage of the wave mechanics of the impinging quanta, then they can be guided into the detection volume such that the momentum and energy information is fully preserved, the potential of which is discussed in the next section.

3. Extending the bandwidth of wave-guiding media via self-assembled metamaterials

If one can inject the incident particle's energy into mechanical vibrational modes, such as the lever modes discussed in (Hammig, 20005) or the whispering-gallery modes discussed in (Zehnpfennig et al., 2011), then one can eschew the charge-conversion process altogether, as well as the inefficiencies inherent to the charge creation and collection processes. Utilizing the wave-mechanics of the radiation proceeds most simply from long wavelength electromagnetic waves, where microwave and optical light guiding and cloaking have already been demonstrated, to the shorter wavelengths that accompany ionizing radiation. The science of guiding electromagnetic waves is aided by the development of metamaterials, which permit one to exercise control over the permittivity and permeability of the transmission medium. If one can reduce the sizes of the nanoscale features in a

metamaterial, then the effective medium approximation can be extended to increasingly small wavelengths such that UV, x-ray, and potentially, gamma-ray wave-guiding can be elicited. Such a development has consequence for not only sensing applications but it also provides an alternative radiation-shielding modality to the existing materials, and provides the promise of light-weight, high efficiency shielding systems.

There has been no *fundamental* advance in the science of nuclear-radiation shielding since the dawn of the nuclear era. Existing shielding materials depend on *particle*-interaction models, in which one maximizes the number of high cross-section scattering sites that can be placed between the radiation source and the protected asset. However, the advent of nanostructured materials provides means through which novel physics can be realized. In particular, they provide a physical pathway through which the wave mechanics of electromagnetic radiation can be controlled via the spatial mapping of the permittivity and permeability. Such control can be realized over electromagnetic waves ranging from microwaves to optical photons. Extending that capability to shorter wavelengths requires either correspondingly smaller nanostructures, or new modalities for controlling the indices of refraction.

Invisibility cloaks generally operate on two operational principles. In the first, transformational optics- in which optical conformal mapping is used to design and grade a refractive index profile- can be used to render an object invisible by precisely guiding the flow of electromagnetic radiation around the object, in a push-forward mapping cloak or a conformal mapping cloak (H. Chen et al., 2010). The underlying mechanism stems from the invariance of Maxwell's equations to coordinate transformations, the effect of which is to only change constitutive parameters and field values. Thus, the space about a cloaked object can be removed from the space that is transformed by the coordinate transformation.

If one utilizes a metamaterial with a negative index of refraction, then one can also cloak an object by cancelling the wave scattering from the target. Optical negative index metamaterials (NIMs) typically require a plasmonic material, which is comprised of a metal-dielectric composite comprised of nanoscale-sized elements. For instance, Valentine et al. utilized a structure consisting of alternating layers of Ag and MgF₂ in a cascaded fishnet structure, in order to realize a 3D optical metamaterial with very low losses (Valentine et al., 2011). The unit cell dimensions were 860 x 565 x 265 nm and the material successfully exhibited the desired refractive index at optical wavelengths of 1200 - 1700 nm; thus, the nanostructural dimensions were approximately one-half to one third of the wavelength. Note that the regular structure of the fishnet structure, shown in Fig. 16b, was patterned using focused ion-beam (FIB) milling, which is capable of precise, nanoscale cutting with high aspect ratios.

Another example is shown in Fig. 16a, in which an optical cloak for the transverse magnetic waveguide mode is comprised of isotropic dielectric materials and delivered broadband and low-loss invisibility in the 1400-1800 wavelength range. The hole diameter shown in Fig. 16a is 110 nm, approximately one-tenth the wavelength, and was again realized with FIB milling.

In fact, most of the cloaking demonstrations to date have used a material-*removal* fabrication modality in which the composite structure is built-up via deposition procedures, and then electron beam lithography or FIB milling is used to realize the structure by etching the underlying composite. Unfortunately, both procedures are slow and costly when implemented over large areas. More importantly, they do not generally allow the precise patterning of materials to the levels required to realize wave optics with x- or gamma-rays.

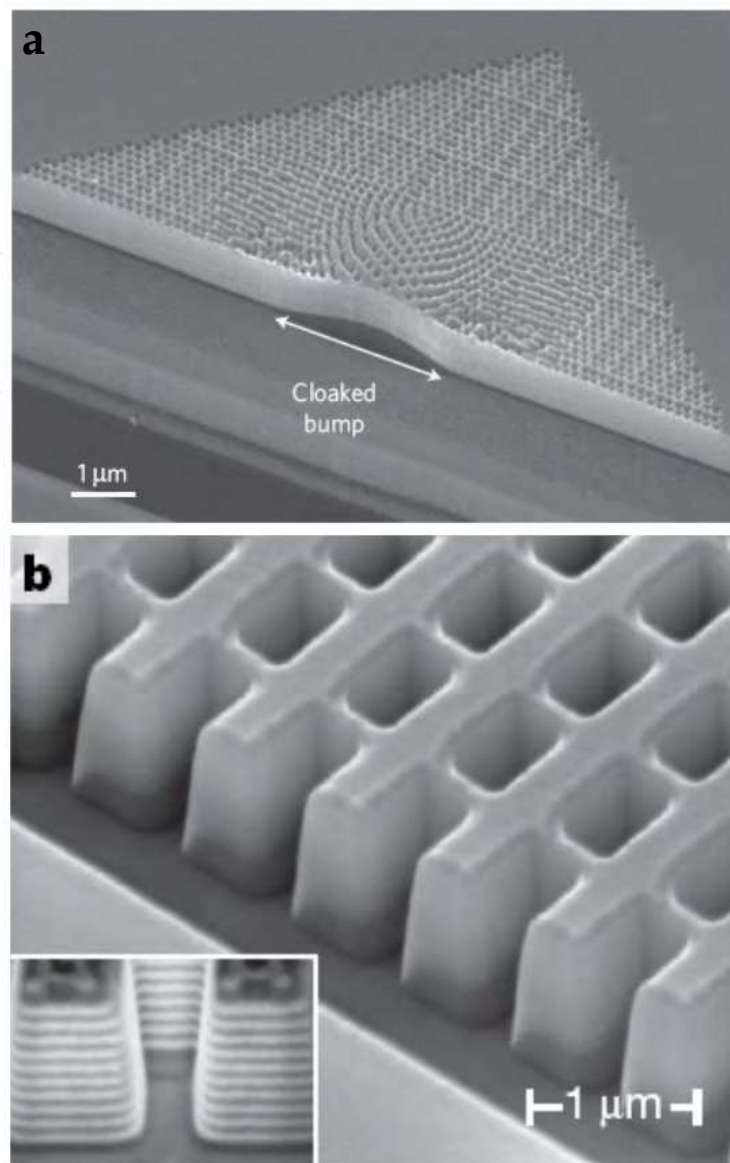


Fig. 16. (a) The carpet cloak design that transforms a mirror with a bump into a virtually flat mirror. Note the gradient index cloak above the bump, the pattern fabricated in a SOI wafer where the Si slab serves as a 2D waveguide. (b) SEM image of fabricated 21-layer fishnet structure, consisting of alternating layers of 30 nm silver and 50 nm magnesium fluoride (Valentine et al., 2011).

That is, the greatest challenge to achieving wave-guiding effects at x- or gamma-ray wavelengths, is that for existing metamaterials, the material loss and fabrication difficulties are substantial. As suggested above, the size of the nanostructure is generally sub-wavelength, so that the index of refraction of the material is governed by the effective medium approximation. The wavelength of a 1 keV x-ray is 1.23 nm; thus, a nanostructured metamaterial must have an ordered nano-crystalline structure in the nanometer range, which is beyond the capabilities of standard e-beam tools, and one must therefore deviate from the material-removal modality.

Fortunately, the desired size-scale can be realized with self-assembly, in which the current lower limit is in this nanometer scale and thus potentially applicable to x-ray cloaking. A

combination of sol preparation and electrophoretic deposition has been used to synthesize a variety of oxide nanorod arrays, such as TiO_2 , SiO_2 , Nb_2O_5 , V_2O_5 , BaTiO_3 , $\text{Pb}(\text{Zr,Ti})\text{O}_3$, Sn-doped In_2O_3 (ITO), and $\text{Sr}_2\text{Nb}_2\text{O}_7$ (Kao, 2004). We have grown nanowires from CdTe and PbSe semiconductors, upon which metallic shells can be deposited. There has been a myriad of different self-assembled nanostructures, but they do not approach the process uniformity and control that accompanies batch-processing methods (cf. Ko et al., 2011), and the deviations in the uniformity would diminish any wave-guiding achieved from a designed array of plasmonic structures of similar size. Nevertheless, some wave guiding can occur from an array of proper materials. Thus, using fabrication techniques similar to that that have been successfully employed to make high-performance charge-conversion devices, one can conceivably change the materials in the nanostructured array in order to exercise control over the wave mechanics of high energy photons.

4. Conclusion

Nanostructured media allow us to measure ionizing radiation with greater precision than can be achieved with single-crystal media because one has greater experimental control over the detector's governing parameters- the size and shape of the nanoparticles- than can be equivalently achieved in a nominally single-crystal media, in which defects and impurities can readily spoil the performance of the sensor. More importantly, one can yield fundamentally superior detection characteristics because one has a mechanism through which the informational processes- such as electron creation- can be controlled relative to the loss processes- such as phonon excitation. Fortunately, this superior physics is also accompanied by a less expensive fabrication modality.

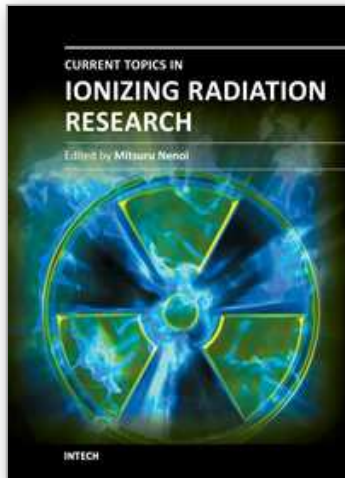
Nanostructured materials have therefore been projected as the next-generation material for the detection of ionizing radiation, the adoption of which depends on overcoming the expected difficulties associated with using a composite material comprised of innumerable interfaces at which information can be lost. As we have shown in this chapter, methods exist that can quench interface trapping so that the promise of the material can be realized today.

5. References

- Bahl, G.; et al., Stimulated optomechanical excitation of surface acoustic waves in a microdevice. *Nat. Commun.* 2:403 doi: 10.1038/ncomms1412 (2011).
- Chen, H.; C. Chan & P. Sheng. Transformation optics and metamaterials, *Nature Materials* Vol. 9, (2010).
- Coe-Sullivan, S.; et al., "Large-Area Ordered Quantum-Dot Monolayers via Phase Separation during Spin Casting", *Adv. Funct. Mater.* 15 (2005).
- Du, H.; et al., Optical properties of colloidal PbSe nanocrystals, *Nano Lett.*, vol. 2, no. 11, pp. 1321-1324, (2002).
- Hammig, M.D; D. K. Wehe and J. A. Nees, , The measurement of sub-brownian lever deflections. *IEEE Trans. Nuc. Sci.* 52, 3005-3011 (2005).
- Hammig, M.D.; G. Kim, Fine Spectroscopy of Ionizing Radiation via a Colloidal Array of Blended PbSe Nanosemiconductors (submitted, 2011).
- Jacobsohn, L.G.; et al., Fluoride Nanoscintillators, *Journal of Nanomaterials*, Vol. 2011 (2011).

- Kim, G.; J. Huang and M.D. Hammig, An Investigation of Nanocrystalline Semiconductor Assemblies as a Material Basis for Ionizing-Radiation Detectors. *IEEE Trans. Nuc. Sci.* 56 841-848 (2009).
- Kim, G; M.D. Hammig, Development of Lead Chalcogenide Nanocrystalline (NC) Semiconductor Ionizing Radiation Detectors. *2009 IEEE Nuc. Sci. Sym. Conf. Record*, 1317-1320 (2009).
- Klassen, N.V.; et al., Advantages and problems of nanocrystalline scintillators, *IEEE Trans. on Nuc. Sci.*, Vol. 55, 1536-1541 (2008).
- Lacy, J; et al., Boron-Coated Straw Detectors: a Novel Approach for Helium-3 Neutron Detector Replacement, *2010 IEEE Nuclear Science Symposium and Medical Imaging Conference (2010 NSS/MIC)*, p 3971-5, (2010).
- Murray, C.B.; et al., Colloidal synthesis of nanocrystals and nanocrystal superlattices, *IBM J. Res. & Dev.*, vol. 45, no. 1, pp. 47-56, Jan. 2001.
- Olkhovets, A.; et al., Size-dependent temperature variation of the energy gap in lead-salt quantum dots, *Phys. Rev. Lett.*, vol. 81, pp. 3539-3542, (1998).
- Remacle, F. et al., Conductivity of 2-D Ag Quantum Dot Arrays: Computational Study of the Role of Size and Packing Disorder at Low Temperatures, *J. Phys. Chem.*, vol. 106, pp. 4116-4126, (2002).
- Rogach, A.L; et al., II-VI semiconductor nanocrystals in thin films and colloidal crystals, *Colloids Surf. A*, vol. 202, iss. 2-3, pp. 135-144, (2002).
- Schaller, R. D., et al., Breaking the phonon bottleneck in semiconductor nanocrystals via multiphonon emission induced by intrinsic nonadiabatic interactions, *Phys. Rev. Lett.*, vol. 95, 196401, (2005).
- Ullom, J.N.; et al., Multiplexed microcalorimeter arrays for precision measurements from microwave to gamma-ray wavelengths. *Nucl. Inst. and Meth. A* 579 161-164 (2007).
- Withers, N.; et al., Lead-iodide-based nanoscintillators for detection of ionizing radiation, *Proc. Of SPIE Vol. 7304*, 73041N (2009).
- Zehnpfennig, J.; et al., Surface optomechanics: calculating optically excited acoustical whispering gallery modes in microspheres, *Optics Express*, vol. 19, 14241 (2011).

IntechOpen



Current Topics in Ionizing Radiation Research

Edited by Dr. Mitsuru Neno

ISBN 978-953-51-0196-3

Hard cover, 840 pages

Publisher InTech

Published online 12, February, 2012

Published in print edition February, 2012

Since the discovery of X rays by Roentgen in 1895, the ionizing radiation has been extensively utilized in a variety of medical and industrial applications. However people have shortly recognized its harmful aspects through inadvertent uses. Subsequently people experienced nuclear power plant accidents in Chernobyl and Fukushima, which taught us that the risk of ionizing radiation is closely and seriously involved in the modern society. In this circumstance, it becomes increasingly important that more scientists, engineers and students get familiar with ionizing radiation research regardless of the research field they are working. Based on this idea, the book "Current Topics in Ionizing Radiation Research" was designed to overview the recent achievements in ionizing radiation research including biological effects, medical uses and principles of radiation measurement.

How to reference

In order to correctly reference this scholarly work, feel free to copy and paste the following:

Mark D. Hammig (2012). Nanoscale Methods to Enhance the Detection of Ionizing Radiation, Current Topics in Ionizing Radiation Research, Dr. Mitsuru Neno (Ed.), ISBN: 978-953-51-0196-3, InTech, Available from: <http://www.intechopen.com/books/current-topics-in-ionizing-radiation-research/the-detection-of-ionizing-radiation-principles-and-practice>

INTECH
open science | open minds

InTech Europe

University Campus STeP Ri
Slavka Krautzeka 83/A
51000 Rijeka, Croatia
Phone: +385 (51) 770 447
Fax: +385 (51) 686 166
www.intechopen.com

InTech China

Unit 405, Office Block, Hotel Equatorial Shanghai
No.65, Yan An Road (West), Shanghai, 200040, China
中国上海市延安西路65号上海国际贵都大饭店办公楼405单元
Phone: +86-21-62489820
Fax: +86-21-62489821

© 2012 The Author(s). Licensee IntechOpen. This is an open access article distributed under the terms of the [Creative Commons Attribution 3.0 License](#), which permits unrestricted use, distribution, and reproduction in any medium, provided the original work is properly cited.

IntechOpen

IntechOpen